Journal of Construction and Engineering Technology
Journal homepage: www.journal.fstu.uz

FORMATION OF MULTIPHASE TURBULENT FLOW IN ROTATING PARTS OF HIGH-PRESSURE PIPES USED FOR WATER SUPPLY TO AGRICULTURAL FIELDS

Oybek Muminov, Shukhrat Utbosarov and Mardon Shoev

Fergana State Technical University, Uzbekistan
*Correspondence: o.muminov@ferpi.uz

Abstract

This article explains the reasons for the occurrence of multi-phase turbulent flow in a curved pipe, and also investigates the phenomenon of cavitation of the generated turbulent flow in formation of multiphase turbulent flow in rotating parts of high-pressure pipes used for water supply to agricultural fields and the factors that cause vibration as a result. The classification of existing approaches to the numerical calculation of turbulent flows is based on the level of detail in the resolution of turbulent fluctuations and their energy spectrum. Given this feature, there are three main approaches (DNS, LES and RANS). In this article, the processes occurring in a bent pipe are studied using the RANS approach from the above approaches. As a result of turbulent flow, a vortex is formed in the pipe, and the effect of these vortices on the pipe has been studied. To study and numerically analyze this problem, we used the Reynolds-averaged system of Navier-Stokes equations, which takes into account the relationships between the phases. The system of Reynolds-averaged Navier-Stokes equations is not closed, and the unified Boussinesq hypothesis is used to close this system. Due to this, unknown terms of the Reynolds equation are formed, which are called Reynolds stresses.

Keywords: Turbulent flow, diffusion, laminar flow, large aggregates, Reynolds stress, Navier-Stokes equations, high-speed deformation.

1. Introduction

If the channel has a transverse slope, then a bend is formed in the flow. The lower part of the cross section of the bend can be straight or curved. In turn, there are many works devoted to the calculation of flow parameters, and their study was carried out under the conditions of an ideal fluid flow. When studying the real, that is, the real flow of a fluid, it is usually assumed that there is only a longitudinal component of the velocity. There are works that also take into account the circulation of the liquid, and the flow, in turn, is considered to be two-dimensional ($u_z = 0$). A very complex turbulent flow occurs inside a curved pipe. Therefore, let us consider modeling of turbulent flows. Turbulent flow in hydromechanics means-that some particles of a fluid move unevenly and unsteadily along a complex trajectory [1], [2]. In this case, the speed of each point of the flow changes in time and is of a pulsating (fast) character. There is a pulsating change in pressure, the density of the compressible fluid changes.

Turbulent flow is characterized by high heat transfer, rapid propagation of chemical reactions, scattering of sound and electromagnetic waves, as well as momentum transfer and, consequently, a high force effect on solids during their rotation. In this case, moving bodies (particles, waves) in turbulent flows encounter great resistance, causing large energy losses.

In turbulent flow, certain masses of a moving fluid are intensively mixed. To determine the turbulence of the flow, the Reynolds number is determined [1].

$$Re_L = U_m L/\nu,$$

where U_m –is the average gas or liquid flow rate, ν is the kinematic viscosity of the gas or liquid, L is the characteristic flow height (for pipes with an internal diameter D).

Immersed Boundary Method (IBM) is an alternative numerical procedure that enables to efficiently handle motions of complex geometry while

Received: 27 December 2025
Revised: 24 January 2026
Accepted: 8 June 2026

https://doi.org/10.24412/2181-4473-2026.4/105

maintaining high accuracy. IBM was first proposed by Peskin to simulate the blood flow in the mitral valve and the heart at two-dimensional (2D) flow and a low Reynolds number[3]. Lagrangian methods employed for particle tracking are conventionally based on the equation of motion for spherical particles at high-Reynolds numbers, as given by Clift[3], also known as Basset–Boussinesq–Oseen (BBO) equation[4].

There are several approaches to modeling turbulent flows. The classification of existing approaches to the numerical simulation of turbulent flows is based on the level of detail in the resolution of turbulent fluctuations and their energy spectrum. Given this feature, there are three main approaches Direct Numerical SimulationLES (DNS), Large Eddy Simulation (LES) and Reynolds Average Navier-Stoks (RANS).In practical applications the flow field is modelled by use of RANS, whereas the resort to DNS [5]–[10] or LES[11]–[15] is still confined to research studies dealing for example with turbulence–particle interactions. Analysis of the various models reveals that for most of the reported applications the Reynolds averaged Navier–Stokes approach is inherently ill-posed and should be transcended by the promising large-eddy simulation concept[16]. Even recently, application of multiphase Computational Fluid Dynamics (CFD) to engineering and real system-scale calculations has been limited to averaged Eulerian-Eulerian formulations coupled with Reynolds-averaged Navier-Stokes (RANS) turbulent flow modelling approaches[16-17]. The dynamics of fluids under strong rotation is a challenging problem in the field of hydrodynamics and magnetohydrodynamics [18], [19].

Turbulent flow can be represented as a set of vortices (vortices) rotating in different directions and in different planes. Large clumps turn into small clumps, and small clumps, i.e., clumps whose size somewhat exceeds the length of the path of free compression of the molecule, convert their energy into viscous thermal energy. This process was first mathematically described by A. N. Kolmogorov and called the energy cascade.

The Navier–Stokes equation and the law of conservation of mass are represented in tensor form as follows [20]:

$$\begin{cases} \rho\dfrac{\partial\overline{u_i}}{\partial t}+\rho\dfrac{\partial\left(\overline{u_i}\,\overline{u_j}\right)}{\partial x_j}=-\dfrac{\partial\overline{p}}{\partial x_i}+\mu\dfrac{\partial^2\overline{u_i}}{\partial x_j\partial x_j}, \\ \dfrac{\partial\overline{u_j}}{\partial x_j}=0, \quad (i,j=1,2,3). \end{cases} \tag{1}$$

The tensor form of the Reynolds equation after applying the Boussinesq conjecture is as follows:

$$\begin{cases} \dfrac{\partial\overline{u_i}}{\partial t}+\dfrac{\partial\left(\overline{u_i}\,\overline{u_j}\right)}{\partial x_j}=-\dfrac{\partial\overline{p}}{\rho\partial x_i}+\dfrac{\partial}{\partial x_j}\left(\left(\nu+\nu_t\right)\dfrac{\partial\overline{u_i}}{\partial x_j}\right), \\ \dfrac{\partial\overline{u_j}}{\partial x_j}=0, \quad (i,j=1,2,3). \end{cases} \tag{2}$$

In the Reynolds equation above, unknown terms are formed, that is, these terms are called Reynolds stresses. Currently, there are many different semi-empirical models for determining Reynolds stresses.

2. Physical Statement of the Problem

The physical formulation of the problem is illustrated in fig. 1.

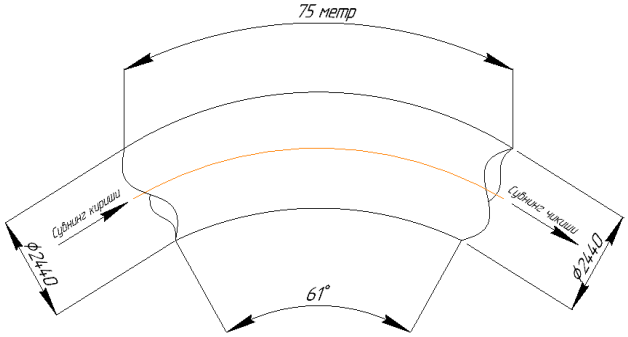


Figure 1. Physical statement of the problem

For the numerical study of this problem, the system of Reynolds-averaged Navier-Stokes equations is used, which takes into account the interaction between the phases [21]. The system of equations does not take into account the forces arising from turbulent migration, Sefman, Magnus (lift force) and the Coriolis effect [22]. Because they are much less than gravity. Thus, for mathematical modeling of the processes of transfer of air bubbles, precipitation and aerosols into the channels, it is sufficient to take into account the force of gravity and the Stokes force of phase interaction.

$$\begin{cases} \dfrac{\partial\overline{U}_j}{\partial x_j}=0, \\ \dfrac{\partial\overline{U}_i}{\partial t}+\overline{U}_j\dfrac{\partial\overline{U}_i}{\partial x_j}=-\dfrac{1}{\rho}\dfrac{\partial p}{\partial x_i}+\dfrac{\partial}{\partial x_j}\left[\nu\left(\dfrac{\partial\overline{U}_i}{\partial x_j}+\dfrac{\partial\overline{U}_j}{\partial x_i}\right)\right]+\dfrac{1}{\rho}\dfrac{\partial}{\partial x_j}\left(-\rho\overline{u'_i u'_j}\right)-\sum_{m=1}^{N}\dfrac{\rho_m}{\rho}k_m\left(\overline{U}_i-\overline{U}p_i\right), \\ \dfrac{\partial\overline{U}p_i}{\partial t}+\overline{U}_j\dfrac{\partial\overline{U}p_i}{\partial x_j}=k_m\left(\overline{U}_i-\overline{U}p_i\right), \\ \dfrac{\partial\rho_m}{\partial t}+\overline{U}p_j\dfrac{\partial\rho_m}{\partial x_j}=D\dfrac{\partial}{\partial x_j}\left[\dfrac{\partial\rho_m}{\partial x_j}+\dfrac{\partial\rho_m}{\partial x_i}\right]. \end{cases} \tag{3}$$

where $\overline{U}_i$ - are the axial, radial and tangential components of the air flow velocity, respectively; $\overline{U}p_i$ - similar velocity components for the m-part of

deposits; $\overline{p}$ - hydrostatic pressure; ρ - gas density; v - its molecular viscosity; $\rho\overline{u'_i u'_j}$ components of the Reynolds stress tensor; ρ_m - mass density of deposits; *km* is the coefficient of air interaction with the *m*-th part of sediments; *N*- is the number of sediment fractions; $D = \frac{\rho}{S_c(\rho+\rho_\rho)}\left(\nu + \left(-\overline{u'v'}\left(\frac{\partial \overline{U}_i}{\partial x_j}\right)^{-1}\right)\right)$ is the diffusion coefficient for the precipitate phase, $Sc = 0.8$ is the Schmidt coefficient.

The interaction coefficient between the phases was determined by the Stokes parameter:

$$k_m = \frac{18\rho v}{\rho_\rho \delta_m^2}.$$

In this expression, ρ_ρ the density of the deposits δ_m is the diameter of the deposits.

The system of Navier-Stokes equations averaged over Reynolds (1) is not closed. To close this system in linear models, the generalized Boussinesq hypothesis is used.

$$-\overline{u_i' u_j'} = v_t\left(\frac{\partial \overline{U}_i}{\partial x_j} + \frac{\partial \overline{U}_j}{\partial x_i}\right) - \frac{2}{3}k\delta_{ij}. \quad (4)$$

Here v_t is turbulent viscosity.

The thesis used the highly acclaimed Spalart-Allmares model. The differential form of this model is as follows [19]:

$$\frac{\partial \tilde{v}}{\partial t} + U_j\frac{\partial \tilde{v}}{\partial x_j} = C_{b1}(1-f_{t2})\tilde{S}\tilde{v} - \left[C_{w1}f_w - \frac{C_{b1}}{k^2}f_{t2}\right]\left(\frac{\tilde{v}}{d}\right)^2 + \frac{1}{\sigma}\left[\frac{\partial}{\partial x_j}\left((v+\tilde{v})\frac{\partial \tilde{v}}{\partial x_j}\right) + C_{b2}\frac{\partial \tilde{v}}{\partial x_i}\frac{\partial \tilde{v}}{\partial x_i}\right]. \quad (5)$$

The turbulent viscosity coefficient is defined as:

$$v_t = \tilde{v}f_{v1}.$$

Additional features and parameters of the model are as follows:

$$f_{v1} = \frac{x^3}{x^3 + c_{v1}^3}, \quad x = \frac{\tilde{v}}{v}, \quad \tilde{S} = \Omega + \frac{\tilde{v}}{k^2 d^2}f_{v2}.$$

$$\Omega = \sqrt{2W_{ij}W_{ij}}$$

$$f_w = g\left[\frac{1+C_{w3}^6}{g^6 + C_{w3}^6}\right], \quad g = r + C_{w2}(r^6 - r),$$

$$f_{v2} = 1 - \frac{x}{1+xf_{v1}}, g = r + c_{w2}(r^6 - r),$$

$$f_{t2} = c_{t3}\exp(-c_{t4}x^2), \qquad r = \min\left[\frac{\tilde{v}}{\tilde{S}k^2 d^2}, 10\right],$$

$$W_{ij} = \frac{1}{2}\left(\frac{\partial U_i}{\partial x_j} - \frac{\partial U_j}{\partial x_i}\right).$$

Here, Ω - is the vortex size, $\tilde{S}$ - is the strain rate, *d* -is the nearest distance to the wall.

Table 1

Model constants

σ_v	k_r	C_{b1}	C_{b2}	C_{v1}	C_{w1}	C_{w2}	C_{w3}	C_{r1}	C_{r2}	C_{r3}
2/3	0.41	0.1335	0.622	7.1	$C_{w1} = \frac{C_{b1}}{k^2} + \frac{1+C_{b2}}{\sigma}$	0.3	2.0	1	12	1

3. The Way to Solve the Problem

The volume controller and the finite difference scheme were used only to solve the equations. Due to the complexity of matching the velocity and pressure fields, the Navier-Stokes and SA equations were used, as well as the continuity equations using the SIMPLE algorithm [23].

The McCormack method [24] is a widely used discretization scheme for the numerical solution of hyperbolic differential equations. This second-order finite difference method was introduced in 1969 by Robert W. McCormack. McCormack's method is simple, straightforward, and easy to program. McCormack's method is widely used in solving hydrodynamic equations. McCormack is especially useful for solving non-linear differential equations such as the Euler and Navier-Stokes equations. The system of equations (1) can be expressed as a matrix.

Predictor

$$\frac{\partial \Phi}{\partial t} + \frac{\partial U\Phi}{\partial x} + \frac{\partial V\Phi}{\partial y} = \frac{\mu}{\rho}\left(\frac{\partial^2 \Phi}{\partial x^2} + \frac{\partial^2 \Phi}{\partial y^2}\right) + \Pi^\Phi. \quad (5)$$

Applying the exact predictor-corrector method to the nonlinear Navier-Stokes and SA equations, we obtain the following difference scheme:

$$\bar{\Phi}_{i,j} = \Phi^n_{i,j} - \Delta t(U^n_{i,j}\frac{\Phi^n_{i+1,j}-\Phi^n_{i,j}}{\Delta x} + V^n_{i,j}\frac{\Phi^n_{i,j+1}-\Phi^n_{i,j}}{\Delta y}) + \Delta t(\frac{\Phi^n_{i,j+1}-2\Phi^n_{i,j}+\Phi^n_{i,j-1}}{\mathrm{Re}\,\Delta y^2} + \frac{\Phi^n_{i+1,j}-2\Phi^n_{i,j}+\Phi^n_{i-1,j}}{\mathrm{Re}\,\Delta x^2} + \Pi^{\Phi}). \quad (6)$$

Corrector

$$\Phi^{n+1}_{i,j} = \frac{1}{2}\left(\begin{array}{l}\bar{\Phi}_{i,j} + \Phi^n_{i,j} - \Delta t(\bar{U}^n_{i,j}\frac{\bar{\Phi}^n_{i,j}-\bar{\Phi}^n_{i-1,j}}{\Delta x} + \bar{V}^n_{i,j}\frac{\bar{\Phi}^n_{i,j}-\bar{\Phi}^n_{i,j-1}}{\Delta y}) + \\ +\Delta t(\frac{\bar{\Phi}_{i,j+1}-2\bar{\Phi}_{i,j}+\bar{\Phi}_{i,j-1}}{\mathrm{Re}\,\Delta y^2} + \frac{\bar{\Phi}_{i+1,j}-2\bar{\Phi}_{i,j}+\bar{\Phi}_{i-1,j}}{\mathrm{Re}\,\Delta x^2} + \Pi^{\Phi})\end{array}\right). \quad (7)$$

Here

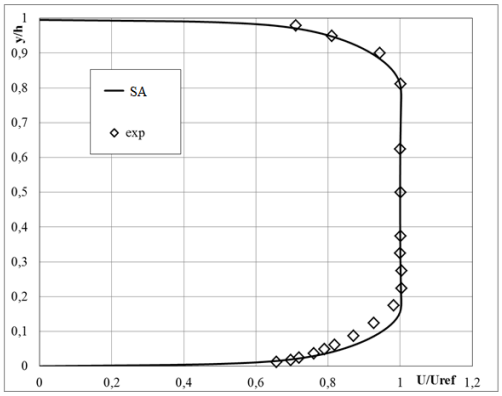
$$\Phi = \begin{pmatrix} U \\ V \\ \tilde{\nu} \end{pmatrix},\ \Pi^{\Phi} = \begin{pmatrix} \frac{\partial p}{\rho \partial x} \\ \frac{\partial p}{\rho \partial y} \\ C_{b1}(1-f_{t2})\tilde{S}\tilde{\nu} - \left[C_{w1}f_w - \frac{C_{b1}}{k^2}f_{t2}\right]\left(\frac{\tilde{\nu}}{d}\right)^2 + \frac{C_{b2}}{\sigma}\left(\left(\frac{\partial \tilde{\nu}}{\partial x}\right)^2 + \left(\frac{\partial \tilde{\nu}}{\partial y}\right)^2\right) \end{pmatrix}.$$

This scheme is considered to be an exact second-order scheme $O\left((\Delta t)^2, (\Delta x)^2, (\Delta y)^2\right)$. The stability of this scheme is defined as follows $\left(\frac{U_{\max}\Delta t}{\Delta x} + \frac{V_{\max}\Delta t}{\Delta y}\right) \le 1$.

4. Model Adequacy

To prove the adequacy of the model, the problem of turbulent motion in a straight pipe was developed. The main goal of working on such a problem is to compare the chosen turbulent model with the experimental problem [25]. In this case, the Reynolds number is 350,000.

On fig. 2 we compare the numerical results with the experimental ones, where the flow has passed into a completely turbulent state and reached a constant value. Here *U* is the fluid velocity at the inlet.



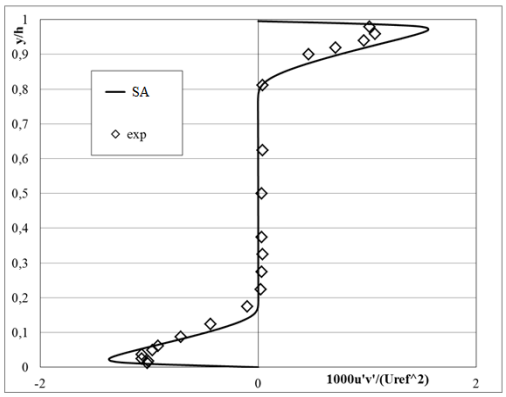


Figure 2. Comparison of numerical results with experimental data:[25] a) longitudinal velocity U, b) Reynolds stresses u'v'

On fig. 3 shows the dependence of the friction coefficient of the pipe on the thickness of the momentum loss. The results of this experiment were taken from Karman-Schoenher [26].

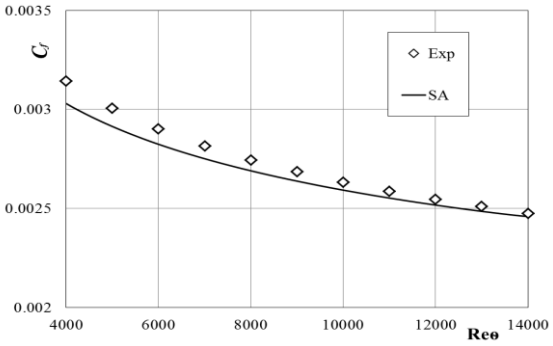


Figure3. Dependence of the coefficient of friction on the Reynolds number of the momentum loss thickness

As can be seen from Figures 2 and 3, the SA model shows very well the flow of fluid inside the pipe.

Returning to the problem in Figure 1, 827702 grids were used to solve this problem, as shown in Figure 4.

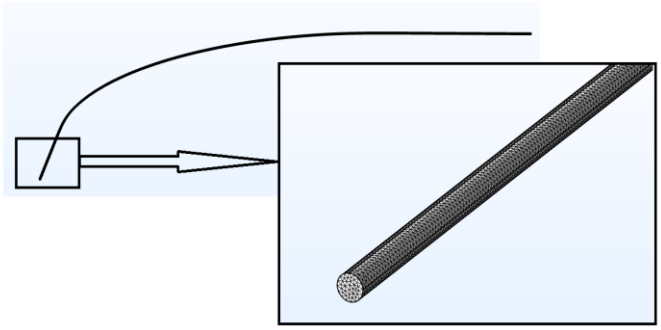


Figure 4. Calculation set for solving the problem

The speed and pressure at the inlet to the pipe are taken from the experiment. On fig. 5 shows the isoline of the fluid pressure Pa in the transverse plane.

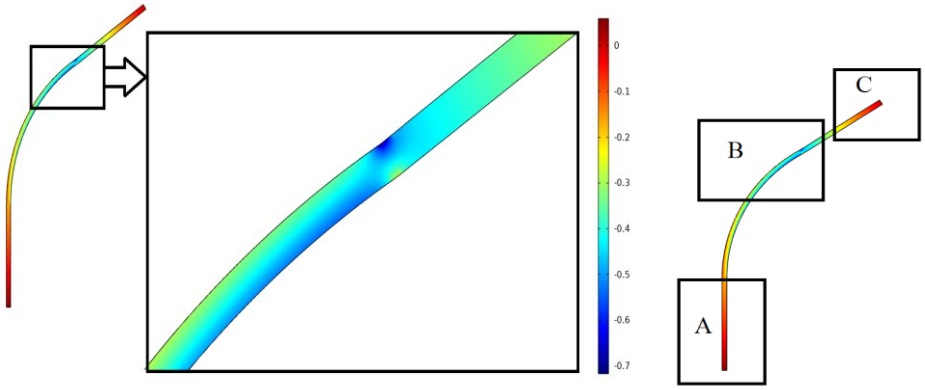
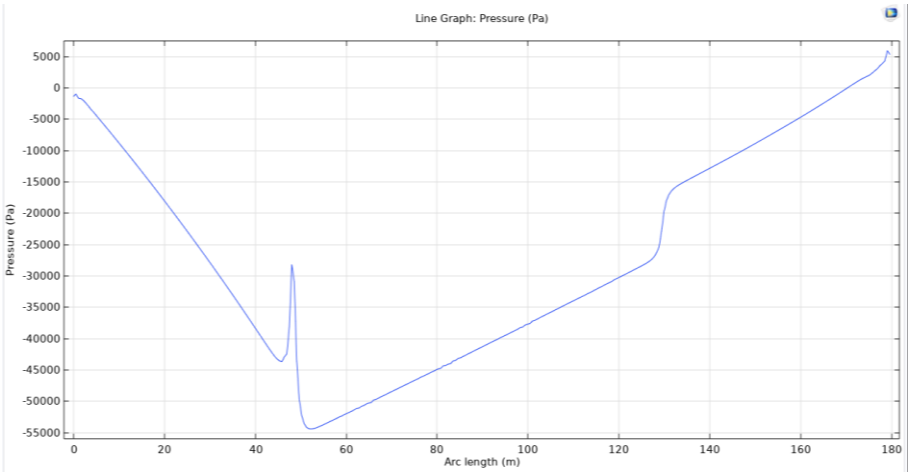


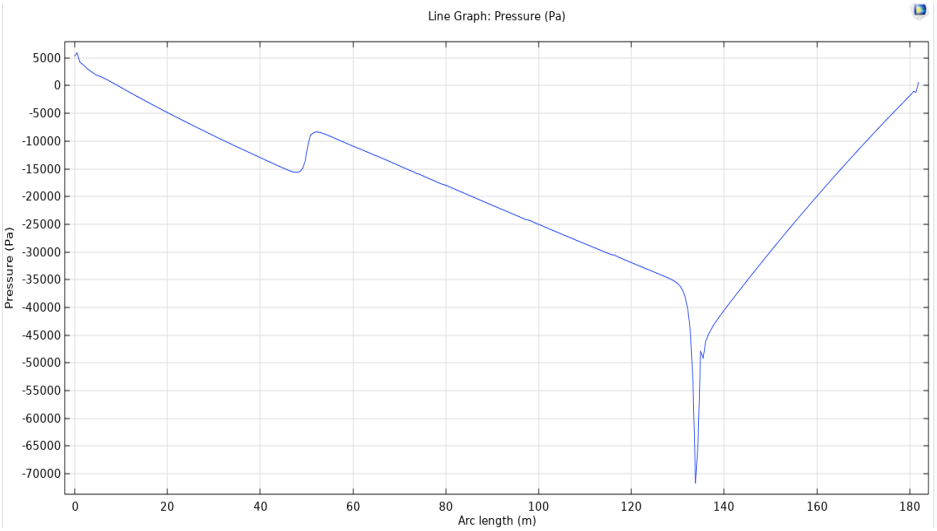
Figure 5. Isoline of fluid pressure (Pa)

So, as you can see from Figure 5, we can divide the total length of the pipe into 3 parts. In section A, we see that the fluid pressure does not change, and in section B, the fluid pressure decreases due to the effect of local resistance. It is in this place that the cold boiling of the liquid occurs, i.e., the phenomenon of cavitation. In the place of low pressure in the liquid, bubbles form, tending to cut along the length of the pipe, and under the action of increased pressure in the cut, the bubbles burst. Therefore, there are noises in the pipes and deformation of the pipe.

On fig. 6 shows the change in pressure along the length of the pipe in the inner and outer sections of the pipe.



a)



b)

Figure 6. Change in pressure along the length of the pipe in a) the inner and b) the outer section of the pipe

On fig. 7 shows the isoline of the longitudinal velocity of the liquid in the transverse plane.

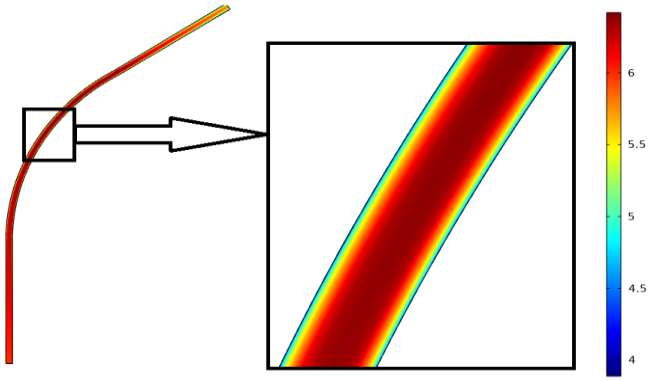


Figure 7. Isoline of the longitudinal velocity of the liquid (m/s)

5. Conclusions

The vibration of the outlet pipes contributes to the transition of the laminar flow regime to the turbulent one at lower values of the lower critical Reynolds number, i.e., causes flow turbulence.

Estimation of vibration effects using the Reynolds vibration number explains the reasons for the discrepancy between the results of similar works by different authors. The resulting analytical formula makes it possible to determine the coefficient of hydraulic friction and the number of cavitations X depending on the vibration parameters. The results of the studies carried out can be used in hydraulic calculations of hydraulic systems under vibration conditions.

An algorithm for estimating fluctuations in the turning part of a turbulent flow in curved pipe has been created, a program and graphs have been obtained. The movement of fluid inside the pipe was modeled using the SA model. With the help of the results obtained, the formation of a turbulent flow in a curved pipe was determined and, as a result, in which sections of the pipe there is a loss of pressure and an increase in velocity. At the points of the curved pipe, the phenomenon of cavitation (cold boiling) is determined, the distribution of pressure and flow is graphically determined.

Using the RANS approach, a mathematical model was created to assess the occurrence of the cavitation phenomenon in a pipe bend. The created mathematical model made it possible to predict in which part of the pipe cavitation will occur.

References

1. Z. M. Malikov and M. E. Madaliev, “Numerical Simulation of Two-Phase Flow in a Centrifugal Separator,” Fluid Dyn., vol. 55, no. 8, pp. 1012–1028, 2020.
2. Madaliev E. et al. Direct numerical simulation of flow in a flat suddenly expanding

3. channel based on nonstationary Navier-Stokes equations //AIP Conference
4. Proceedings. – AIP Publishing, 2023. – Т. 2612. – №. 1.
5. Navruzov, D. P., Madaliev, M. E., Pulatov, T. R., Juraev, S. R., & Boltayev, S. A. (2023, March). Direct numerical simulation of flow in a flat channel with a rectangular step based on the nonstationary Navier-Stokes equations. In AIP Conference Proceedings (Vol. 2612, No.1). AIP Publishing
6. C. S. Peskin, "Flow patterns around heart valves: a numerical method," J. Comput. Phys., vol. 10, no. 2, pp. 252–271, 1972.
7. R. Clift, J. R. Grace, and M. E. W. Bubbles, "drops and particles Academic press," New York, 1978.
8. C. T. Crowe, T. R. Troutt, and J. Chung, "Numerical models for two-phase turbulent flows," Annu. Rev. Fluid Mech., vol. 28, no. 1, pp. 11–43, 1996.
9. K. D. Squires and J. K. Eaton, "Particle response and turbulence modification in isotropic turbulence," Phys. Fluids A Fluid Dyn., vol. 2, no. 7, pp. 1191–1203, 1990.
10. C. Li, A. Mosyak, and G. Hetsroni, "Direct numerical simulation of particle-turbulence interaction," Int. J. Multiph. Flow, vol. 25, no. 2, pp. 187–200, 1999.
11. A. M. Ahmed and S. Elghobashi, "On the mechanisms of modifying the structure of turbulent homogeneous shear flows by dispersed particles," Phys. Fluids, vol. 12, no. 11, pp. 2906–2930, 2000.
12. B. L. Sawford and P. K. Yeung, "Lagrangian statistics in uniform shear flow: Direct numerical simulation and Lagrangian stochastic models," Phys. Fluids, vol. 13, no. 9, pp. 2627–2634, 2001.
13. F. Yeh and U. Lei, "On the motion of small particles in a homogeneous isotropic turbulent flow," Phys. Fluids A Fluid Dyn., vol. 3, no. 11, pp. 2571–2586, 1991.
14. Q. Wang and K. D. Squires, "Large eddy simulation of particle-laden turbulent channel flow," Phys. Fluids, vol. 8, no. 5, pp. 1207–1223, 1996.
15. V. Armenio, U. Piomelli, and V. Fiorotto, "Effect of the subgrid scales on particle motion," Phys. Fluids, vol. 11, no. 10, pp. 3030–3042, 1999.
16. M. Boivin, O. Simonin, and K. D. Squires, "On the prediction of gas–solid flows with two-way coupling using large eddy simulation," Phys. Fluids, vol. 12, no. 8, pp. 2080–2090, 2000.
17. N. Okong'o and J. Bellan, "A priori subgrid analysis of temporal mixing layers with evaporating droplets," Phys. Fluids, vol. 12, no. 6, pp. 1573–1591, 2000.
18. D. Lakehal, "On the modelling of multiphase turbulent flows for environmental and hydrodynamic applications," Int. J. Multiph. Flow, vol. 28, no. 5, pp. 823–863, 2002.
19. A. Prosperetti and G. Tryggvason, Computational methods for multiphase flow. Cambridge university press, 2009.
20. H. P. Greenspan, "The theory of rotating fluids," Massachusetts Inst of Tech Cambridge Dept of Mathematics, 1968.
21. P. A. Davidson, Turbulence in rotating, stratified and electrically conducting fluids. Cambridge University Press, 2013.
22. L. G. Loitsyansky, "The mechanics of fluid and gas, Moscow, Science," Mexanika jidkocti i gaza, Moscow, Nauk., p. 840, 1987.
23. P. R. Spalart and A. Leonard, "Direct numerical simulation of equilibrium turbulent boundary layers," in Turbulent Shear Flows 5: Selected Papers from the Fifth International Symposium on Turbulent Shear Flows, Cornell University, Ithaca, New York, USA, August 7–9, 1985, 1987, pp. 234–252.
24. S. Patankar, "Numerical heat transfer and fluid flow, Ser," Coputational Methods Mech. Therm. Sci, pp. 1–197, 1980.
25. R. W. MacCormack, "The effect of viscosity in hypervelocity impact cratering," J. Spacecr. Rockets, vol. 40, no. 5, pp. 757–763, 2003.
26. M. E. U. Madaliev, Z. E. Abdulkhaev, N. E. Toshpulatov, and A. A. Sattorov, "Comparison of finite-difference schemes for the first order wave equation problem," in AIP Conference Proceedings, 2022, vol. 2637, no. 1, p. 40022.
27. NASA Langley Research Center, "Turbulence modeling Resource."
28. K. E. Schoenherr, "Resistance of flat surfaces moving through a fluid," Trans. Soc. Nav. Arch. Mar. Eng., pp. 279–313, 1932.
29. Z. Abdulkhaev, M. Madraximov, A. Arifjanov, and N. Tashpulotov, "Optimal methods of controlling centrifugal pumps," in AIP Conference Proceedings, 2023, vol. 2612, no. 1, p. 30004.
30. Z. Abdulkhaev, M. Madraximov, J. Orzimatov, and A. Abdurazaqov, "Transition processes during the start-up of the pumping unit of HAPP," 2023.
31. Shoyev, M. A., Ibroximov, A. R., Madaliev, M. E., Dusiyorov, J. J., Rayimqulov, O. Q., & Ismatov, M. N. (2023). Numerical study of modified centrifugal cyclone. In E3S Web of Conferences (Vol. 401, p. 01036). EDP Sciences.
32. Madaliev, E., Madaliev, M., Tursunaliev, M., Shoev, M., & Tashpulatov, N. (2023, March). Direct numerical simulation of flow in a flat suddenly expanding channel based on nonstationary Navier-Stokes equations. In AIP Conference Proceedings (Vol. 2612, No. 1). AIP Publishing.
33. Madaliev, E., Madaliev, M., Mullaev, I., Sattorov, A., & Ibrokhimov, A. (2023, March). Numerical simulation of the layer mixing problem based on a new two-fluid turbulence model. In AIP Conference Proceedings (Vol. 2612, No. 1). AIP Publishing.
34. Malikov, Z. M., & Madaliev, M. E. (2022). Numerical simulation of separated flow past a square cylinder based on a two-fluid turbulence model. Journal of Wind Engineering and Industrial Aerodynamics, 231, 105171.
35. Malikov, Z. M., & Madaliev, M. E. (2021). Numerical study of a swirling turbulent flow through a channel with an abrubt expansion. Vestnik Tomskogo

Gosudarstvennogo Universiteta. Matematika i Mekhanika, (72), 93-101.

36. Malikov, Z. M., Mirzoev, A. A., & Madaliev, M. (2022). Numerical simulation of the mixing layer problem based on a new two-fluid turbulence model. Journal of Computational Applied Mechanics, 53(2), 282-296.
37. Malikov Z.M., Navruzov D.P., Adilov K., Jurayev S,R. Numerical study of a circular jet based on a modern turbulence model // «Computer Applications for Management and Sustainable Development of Production and Industru» (CMSD2021). doi:10.1117/12.2631607.
38. Malikov Z.M., Madaliyev M.E., Navruzov D.P., Adilov K. Numerical study of an axisymmetric jet based on a new turbulence model // International Scientific Conference on Actual Problems of Applied Mechanics, AIP Conference Proceedings. DOI.org/10.1063/5.0118473.
39. Z.M. Malikov., D.P. Navruzov., X. Djumayev. Models results Comparison of different approaches to turbulence for flow past a heated flat plate" E3S Web of Conferences 264, 01008 (2021) https://doi.org/10.1051/e3sconf/202126401008
40. B.M. Kholboev, D.P. Navruzov, D.S. Asrakulova, N.R. Engalicheva and A.A. Turemuratova. Comparison of the results for calculation of vortex currents after sudden expansion of the pipe with different diameters // Int. J. of Applied Mechanics and Engineering, 2022, vol.27, No.2, pp.115-123. DOI: 10.2478/ijame-2022-0023.
41. Ibrokhimov A. I. et al. NUMERICAL SIMULATION OF SEPARATE FLOW AROUND A HEATED SQUARE CYLINDER //Proceedings of the 6th International Conference on Future Networks & Distributed Systems. – 2022. – С. 23-26.
42. Arifjanov, A.M., Sattorov, A.X., Atakulov, D., Iminov, I.X. Method of calculation of the flow motion model in water intake facilities (2023) IOP Conference Series: Earth and Environmental Science, 1231 (1), № 012060. DOI: 10.1088/1755-1315/1231/1/012060